

Supplement of Atmos. Chem. Phys., 15, 12681–12703, 2015
<http://www.atmos-chem-phys.net/15/12681/2015/>
doi:10.5194/acp-15-12681-2015-supplement
© Author(s) 2015. CC Attribution 3.0 License.



Atmospheric
Chemistry
and Physics
Open Access
EGU

Supplement of

Radiative forcing and climate response to projected 21st century aerosol decreases

D. M. Westervelt et al.

Correspondence to: D. L. Mauzerall (mauzeral@princeton.edu) and D. M. Westervelt (danielmw@princeton.edu)

The copyright of individual parts of the supplement might differ from the CC-BY 3.0 licence.

S1. RCP air pollution policy

RCP4.5, developed by the Global Change Assessment Model (GCAM), relates air pollution control levels to relative affluence as measured by GDP based on purchasing power parity (PPP). PPP-based GDP involves scaling the per capita GDP by average prices of a collection of goods (including from the service and investment industries). This is an improved estimate of relative income compared to simple per capita GDP, since it controls for different market exchange rates that are known to underestimate the value of incomes in developing countries (Smith et al., 2005). RCP4.5 uses a logistic curve functional form to relate future emission control with PPP-based GDP (details found in Smith et al. 2005). Other scenarios use similar methods. For example, RCP8.5, developed by the Model for Energy Supply System Alternatives and their General Environmental impacts (MESSAGE), bases its relationship on GDP normalized by market exchange rates (MER) rather than PPP (Riahi et al., 2007) as well as a different functional form, which we discuss below. The authors as well as other studies note that the emissions outcomes are not significantly affected by the use of MER over PPP for GDP, despite PPP-based GDP being the recommended metric when practical and available. (Gruebler and Nakicenovic, 2004; Manne et al., 2005).

Coal use in RCP8.5 is expected to increase by an order of magnitude by 2100. While this clearly makes RCP8.5 the highest CO₂ emissions scenario, this is not necessarily the case for air pollutants. Control measures for air pollutant emissions such as liquid fuel sulfur content limits, use of low sulfur coal, use of electrostatic precipitators, improved cooking stove technology, and other policies are embedded into RCP8.5. It is assumed that present and planned environmental legislation (in the form of the measures discussed above) will be successfully implemented in all regions by 2030. Beyond 2030, an environmental Kuznets curve is used to represent the idea that future wealth will lead to increased environmental regulation, with GDP levels (MER-based, as discussed above) of \$5000/capita serving as the turning point for stricter air pollution control. These assumptions and features of RCP8.5 result in a major decoupling between CO₂ and air pollutant emissions (Riahi et al., 2011).

Each of the RCPs also includes climate policy (or mitigation) measures manifested as improvements in energy efficiency, replacement of fossil fuel usage with renewable and nuclear energy, and development of carbon capture and storage. The exception is RCP8.5 which contains no climate mitigation but does include stringent air pollution measures as described above (Riahi et al., 2011). Many of these climate policies also contribute to reductions in aerosols and their precursors. For example, replacement of coal-fired power plants, the largest anthropogenic SO₂ source, with renewable or nuclear energy will significantly reduce sulfate aerosol formation from SO₂.

S2. Aerosol optical depth

S2.1 Past, present, and future trends in aerosol optical depth

Figure S3 shows the globally averaged historical and future time series for aerosol optical depth (AOD) at 550 nm wavelength for sulfate, black carbon, organic carbon, and their sum. BC and sulfate AOD are partitioned using their respective mass fractions, with sulfate assumed to be pure ammonium sulfate. Sulfate, BC, and OC AOD trends are well correlated with emissions trends, with correlation coefficients ranging from 0.7 to 0.9 for each species and each RCP (not shown). By 2100, sulfate AOD is projected to decrease by 50% from 2005 levels in RCP2.6, 40% in RCP4.5 and RCP6, and 31% in RCP8.5. As with emissions, this arrangement of overall decrease aligns with the extent of climate policy embedded in each of the RCPs. The upper right (lower left) panel of Fig. S3 shows a brief spike in BC (and OC) AOD in the beginning of the 21st century in RCP2.6, which is consistent with emissions projections for BC (Fig. 2, main text). However, the same spike is visible in AOD in the fixed 2005 emissions simulations (RCP2.6_F, dashed lines in Fig. S3) for BC and OC, suggesting that factors other than emissions, such as temperature and rainfall patterns, are driving the AOD increases. RCP6 BC and OC AOD are projected to decrease the least of all the RCPs and even increase in the case of OC AOD, whereas AOD in RCP8.5, RCP2.6, and RCP4.5 decrease more monotonically. Sea salt and dust aerosols are relatively constant and do not vary by more than 2% and 15% respectively over the time period of simulation (1860-2100), indicating little meteorologically-driven variation in natural aerosols.

In each RCP for each species, aerosol optical depth is projected to increase in each of the fixed 2005 aerosol emission simulations (RCPx.x_2005AER, dashed lines in Fig. S3). For example, RCP8.5_2005AER total AOD (sum of sulfate, black carbon, and organic carbon) increases by roughly 20% by the end of the century, which is almost the same amount that RCP8.5 (time-varying simulations) decrease by 2100 (30%). The increase is smaller for the rest of the RCPs: 8% for RCP6, 5% in RCP4.5, and 2% in RCP2.6. The order of AOD increases is consistent with the magnitude of greenhouse-gas driven climate change in each of the RCPs (i.e., RCP8.5 projects the highest warming, RCP2.6 projects the lowest). The reason for this AOD increase is not increasing emissions (since they are held fixed), but instead feedbacks of meteorology on aerosol burdens. In particular, temperature is projected to increase drastically as a result of anthropogenic greenhouse warming (see Fig. 6, main text), and higher temperatures may lead to larger burden by increasing the reaction rates of aerosol-forming reactions, such as sulfur dioxide oxidation. Additionally, decreases in the wet deposition efficiency, which can occur despite an increase in precipitation intensity, may lead to increases in aerosol optical depth (particularly sulfate AOD) (Fang et al. 2011). This is discussed in more detail in Sect. 4.1.1. A particularly striking example of the impact of meteorological factors on AOD can be seen in RCP6 OC AOD, in which case both the RCP6 and RCP6_2005AER simulations have nearly identical OC AOD values for the entirety of the 21st century, suggesting that the trend in OC emissions is not responsible for the AOD increases.

S2.2 Magnitude of aerosol decreases compared to 2005 levels

Figure S4 shows the globally averaged change in aerosol AOD for the 21st century due to projected emission changes in each of the RCPs (Figs. 2 and S3). The trends plotted here are AOD differences between the time-varying aerosol simulations (RCPx.x) and the constant emissions simulations (RCPx.x_2005AER) for each year. Shaded areas represent the range of AOD changes in each of the ensemble members, while solid lines are ensemble means. Since emissions (Fig. 2, main text) and AOD (Fig. S3) mostly decrease over the 21st century globally for each of the RCPs and for each aerosol species, Fig. S3 also mostly shows downward trends. As emissions decrease, the differences in

AOD between the time-varying and fixed aerosol emissions cases get larger in magnitude. For instance, by the end of the century, sulfate AOD will be about 0.034 less in the case with decreasing emissions than in the fixed 2005 emissions levels. This compares very well with many of the other global modeling studies; for example, Levy et al. (2013) reports an AOD change of -0.032 and Rotstayn et al. (2013) reports a total AOD decline of around -0.05, comparable to our total anthropogenic value of -0.04. AOD difference estimates for each RCP (i.e., RCP_{x.x} – RCP_{x.x_2005AER}) for a five-year average (2096-2100) are tabulated in Table 3 (main text). BC and OC AOD values generally decrease as well, with the exception of RCP6 for OC, which hardly changes for the entire century (Fig. S4, Table 3). As explained above, both RCP6_2005AER and RCP6 increase together throughout the century with little difference between the two scenarios, due to temperature changes and changes in aerosol wet deposition lifetimes. Similarly, the same reasoning applies to the RCP8.5 OC differences in Fig. S4, which are negative throughout the century, resulting from the difference between the roughly constant OC AOD time series for RCP8.5 and the large increase in OC AOD of RCP8.5_2005AER (Fig. S3).

With the notable exception of OC AOD and to some extent BC AOD, emission-driven changes in globally averaged AOD are similar in each RCP throughout the 21st century. The end of century values for sulfate AOD changes in particular do not vary by more than 10%, although there are significant deviations in the middle of the century, owing to specific features of each pathway. For example, the stringent climate policy of RCP2.6 is evident in the middle of the 21st century as RCP2.6 sulfate AOD decreases more rapidly than the others, as is the mid-century increase in coal as a primary energy supply in RCP6. Global OC AOD differences are more varied than for sulfate, due to the larger variation in land-use policy than in energy policy. However, since sulfate dominates the total AOD amount, the spread in the sum of sulfate, BC, and OC resembles sulfate more than it does OC. In fact, the end-of-century (2096-2100 five year average) total AOD change in RCP8.5, RCP4.5, and RCP2.6 are virtually identical at around -0.04, with RCP6 being only 20% different than the other three scenarios.

Table S1: Regional average changes in aerosol optical depth, radiative forcing, and climate response for RCP4.5 due to aerosol effects only at the end of the 21st century. Values represent differences between RCP simulations and fixed 2005 simulations (RCP4.5 – RCP4.5_2005AER). Region definitions are in Fig. 1 of the main text.

	SO ₄ AOD	BC AOD	OC AOD	RF (W m ⁻²)	T (K)	P (mm day ⁻¹)	LWP (g m ⁻²)	R _{eff} (μm)
NM	-0.036	-0.0007	-0.0005	1.61	1.73	0.054	-0.703	0.656
SM	-0.023	-0.0024	-0.014	1.19	0.86	-0.009	-1.56	0.672
EA	-0.156	-0.010	-0.023	3.21	1.36	0.352	-4.10	2.12
SA	-0.135	-0.0086	-0.049	4.66	0.99	0.380	-4.44	1.56
EU	-0.082	-0.0039	-0.010	2.02	1.45	0.024	-3.51	1.09
RU	-0.047	-0.0016	-0.0023	1.60	1.75	0.161	1.31	0.998
AU	-0.012	-0.0004	-0.0024	-0.006	0.78	-0.183	-2.34	0.56
AF	-0.035	-0.002	-0.012	1.41	0.86	0.036	-0.821	0.914
ME	-0.072	-0.0016	-0.008	-0.11	1.43	0.016	-1.59	2.20

Table S2: Regional average changes in aerosol optical depth, radiative forcing, and climate response for RCP6.0 due to aerosol effects only at the end of the 21st century. Values represent differences between RCP simulations and fixed 2005 simulations (RCP6 – RCP6_2005AER). Region definitions are in Fig. 1 of the main text.

	SO ₄ AOD	BC AOD	OC AOD	RF (W m ⁻²)	T (K)	P (mm day ⁻¹)	LWP (g m ⁻²)	R _{eff} (μm)
NM	-0.046	-0.0011	.000043	2.10	1.55	0.14	0.322	0.72
SM	-0.022	-0.0006	0.001	1.00	0.71	-0.041	-1.56	0.444
EA	-0.12	-0.0084	-0.015	2.40	1.05	0.270	-2.49	1.55
SA	-0.094	-0.0059	-0.0097	2.63	0.76	0.267	-1.92	0.895
EU	-0.092	-0.0046	-0.0074	2.87	1.64	0.055	-3.93	1.28
RU	-0.042	-0.0015	-0.0003	2.19	1.71	0.120	1.40	0.93
AU	-0.019	-0.0002	0.0003	0.50	0.53	-0.045	-1.07	0.67
AF	-0.052	0.00011	0.0062	1.65	0.88	0.074	-0.93	0.93
ME	-0.074	-0.0021	-0.004	0.59	1.07	0.049	-0.499	1.95

Table S3: Regional average changes in climate response for CM3w RCP8.5 due to aerosol effects only at the end of the 21st century. Values represent differences between RCP simulations and fixed 2005 simulations (CM3w_RCP8.5 – CM3w_RCP85_2005AER). Region definitions are in Fig. 1 of the main text.

	T (K)	P (mm day ⁻¹)	LWP (g m ⁻²)	R _{eff} (μm)
NM	1.07	0.04	0.022	0.54
SM	0.40	0.10	-0.24	0.43
EA	0.79	0.19	-1.08	1.58
SA	0.60	0.38	-0.90	1.05
EU	0.72	-0.02	-1.43	1.08
RU	0.81	0.08	0.61	0.78
AU	0.47	0.04	1.30	1.30
AF	0.77	-0.05	-0.82	0.50
ME	1.10	-0.07	-1.40	1.57

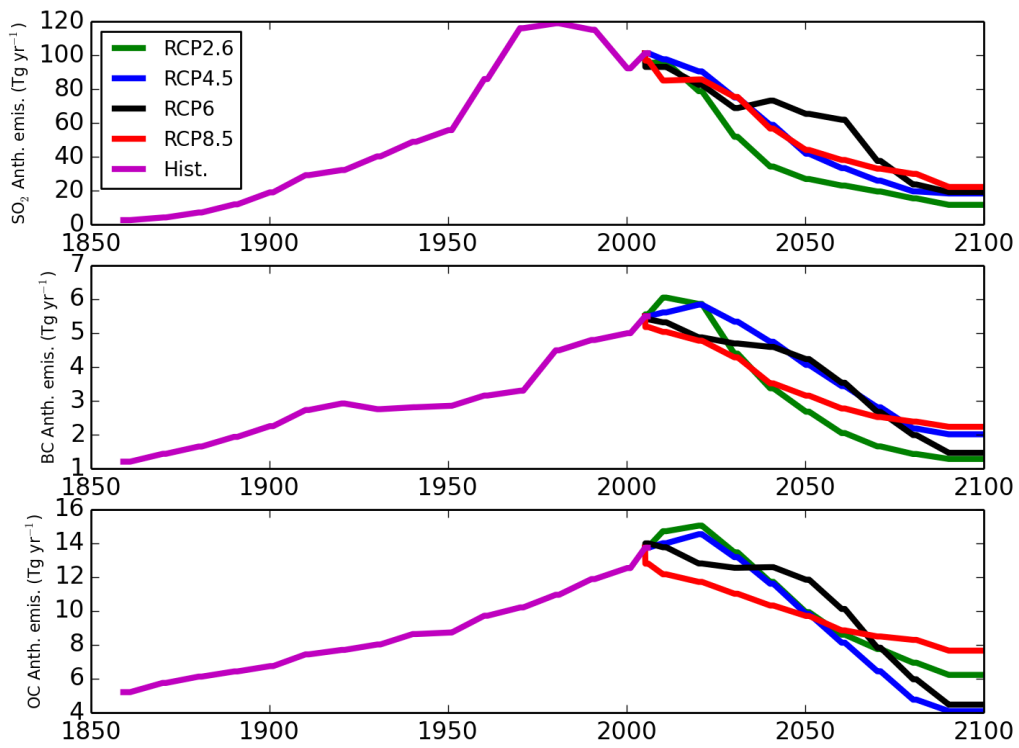


Fig S1: Global average historical and future anthropogenic-only emissions trajectories for sulfur dioxide, black carbon, and organic carbon.

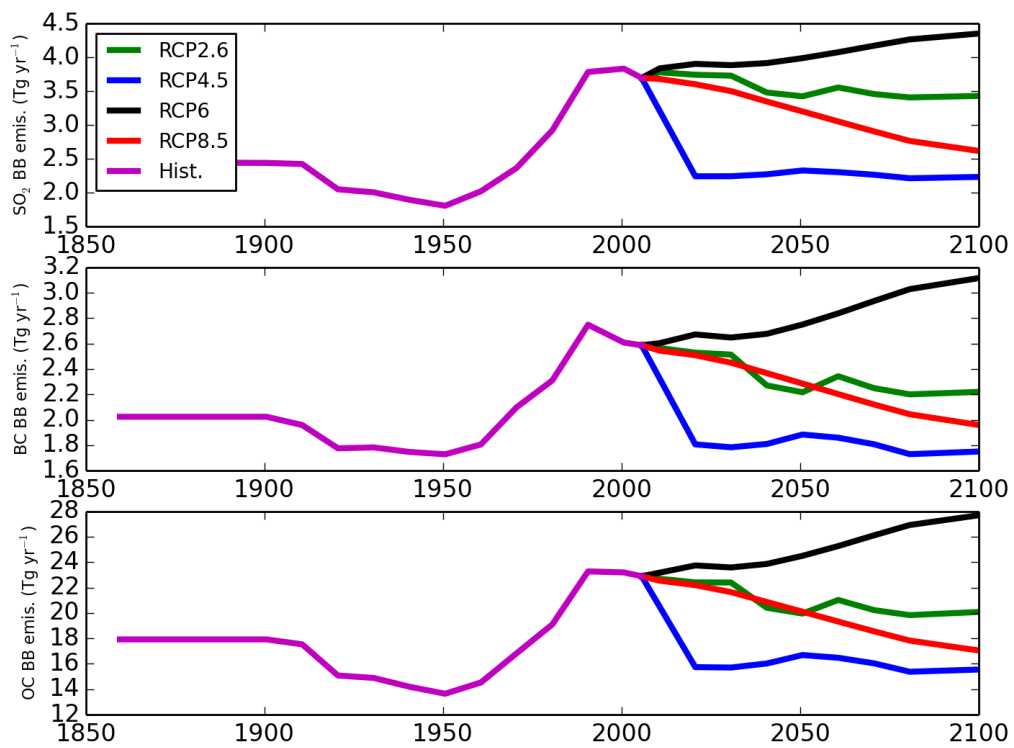


Fig S2: Global average historical and future biomass burning-only emissions trajectories for sulfur dioxide, black carbon, and organic carbon.

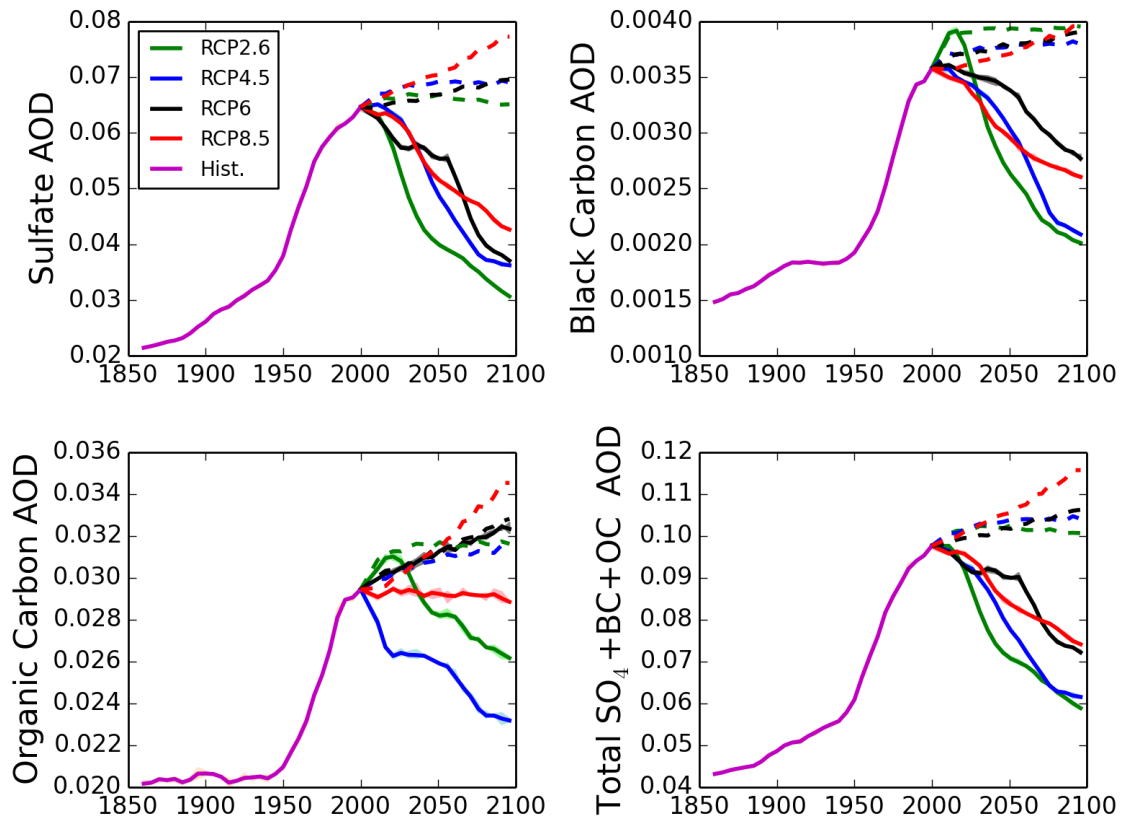


Figure S3: Globally averaged trends in aerosol optical depth (at 550 nm wavelength) from 1860-2100 for each RCP. Upper left: Sulfate, upper right: Black carbon, bottom left: organic carbon, bottom right: sum of sulfate, BC, and OC. Shaded light colors represent the range of the three ensemble members, solid lines are the ensemble means for the RCPx.x time-varying simulations. Dashed lines are the ensemble means for the RCPx.x_2005AER control simulations with constant 2005 aerosol emissions (ensemble range not shown).

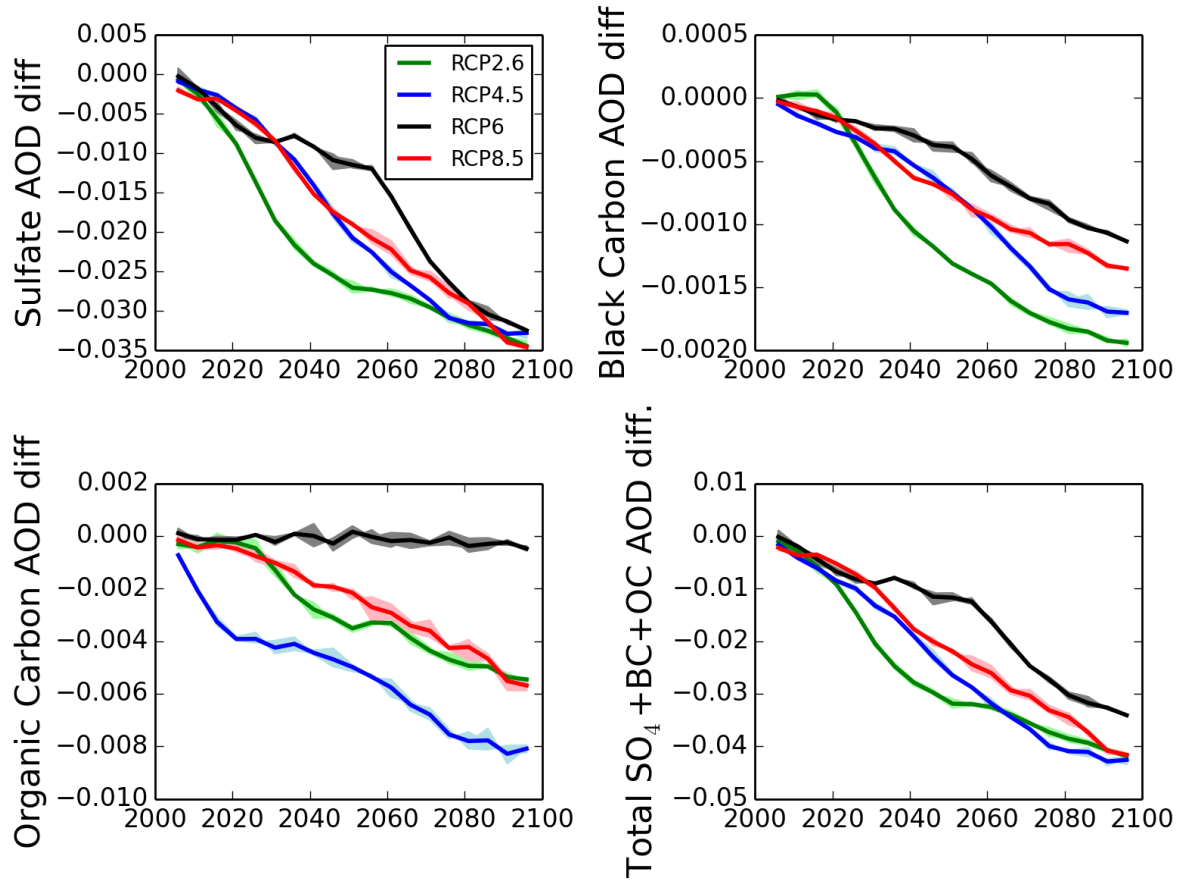


Figure S4: Globally averaged trends in aerosol optical depth (550 nm) anomalies from 2005-2100 for each RCP. Values represent differences between the projected RCP aerosol optical depth and the fixed 2005 aerosol emissions case (base case). Shaded light colors represent the range of the three ensemble members, solid lines are the ensemble means for the RCPx.x time-varying simulations.

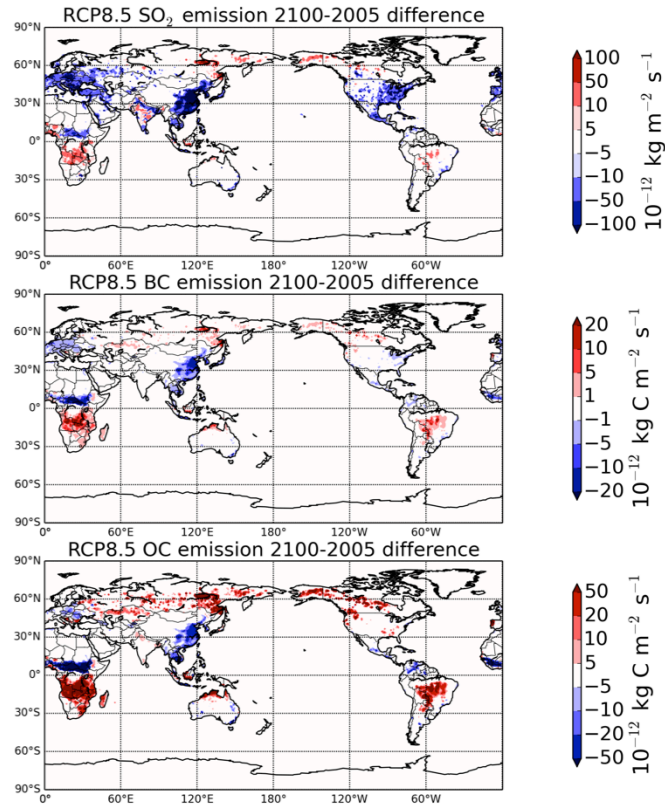


Figure S5: Change in total (anthropogenic + biomass burning) annual emissions in 2100 compared to 2005. Top panel: SO₂ ($10^{-12} \text{ kg m}^{-2} \text{ s}^{-1}$); middle: black carbon ($10^{-12} \text{ kg C m}^{-2} \text{ s}^{-1}$); bottom: organic carbon ($10^{-12} \text{ kg C m}^{-2} \text{ s}^{-1}$)

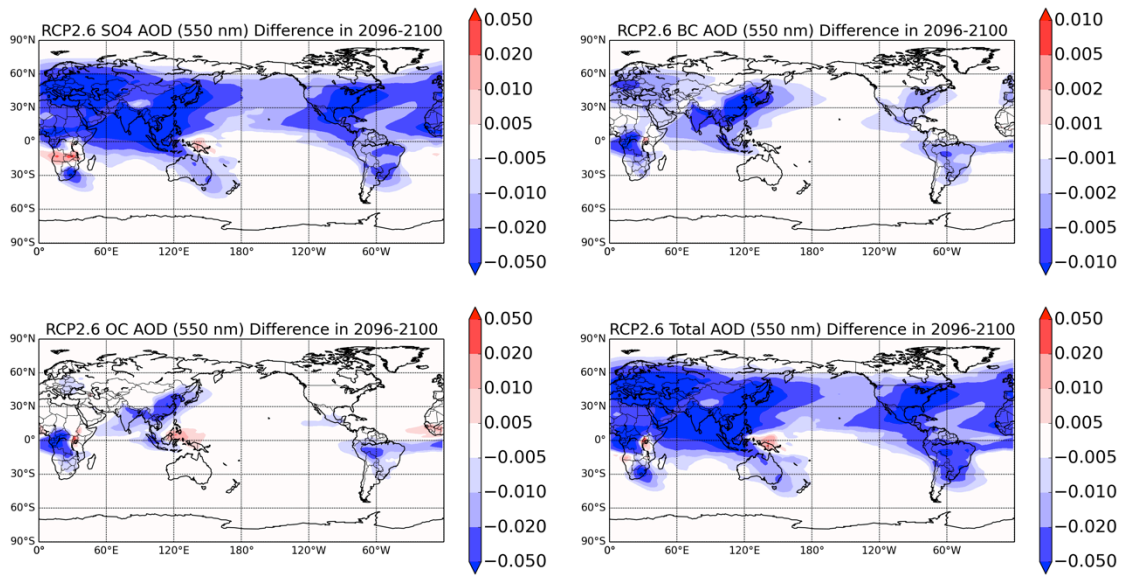


Figure S6: Anomalies in aerosol optical depth for 2096-2100 five-year average for RCP2.6. Values represent differences between the projected RCP aerosol optical depth and the fixed 2005 aerosol emissions case (base case). Note the different scale for BC AOD.

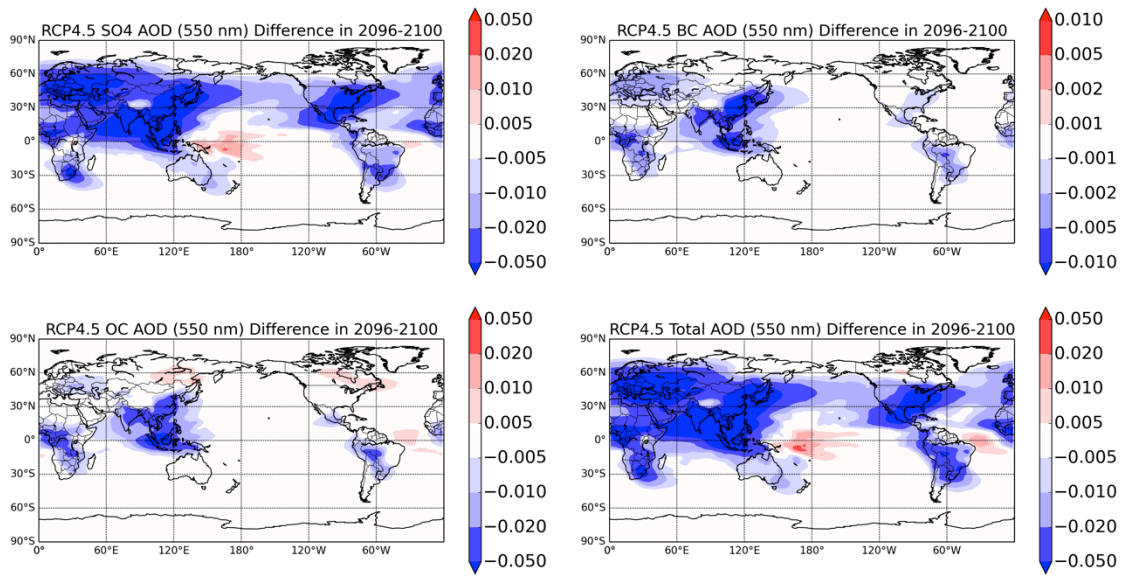


Figure S7: Anomalies in aerosol optical depth for 2096-2100 five-year average for RCP4.5. Values represent differences between the projected RCP aerosol optical depth and the fixed 2005 aerosol emissions case (base case). Note the different scale for BC AOD.

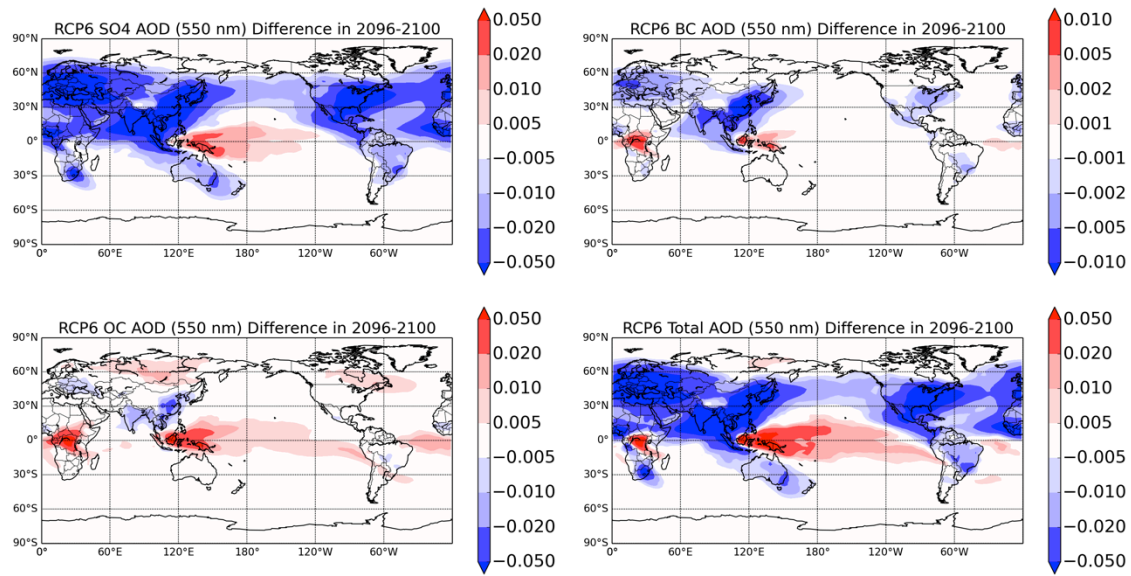


Figure S8: Anomalies in aerosol optical depth for 2096-2100 five-year average for RCP6. Values represent differences between the projected RCP aerosol optical depth and the fixed 2005 aerosol emissions case (base case). Note the different scale for BC AOD.

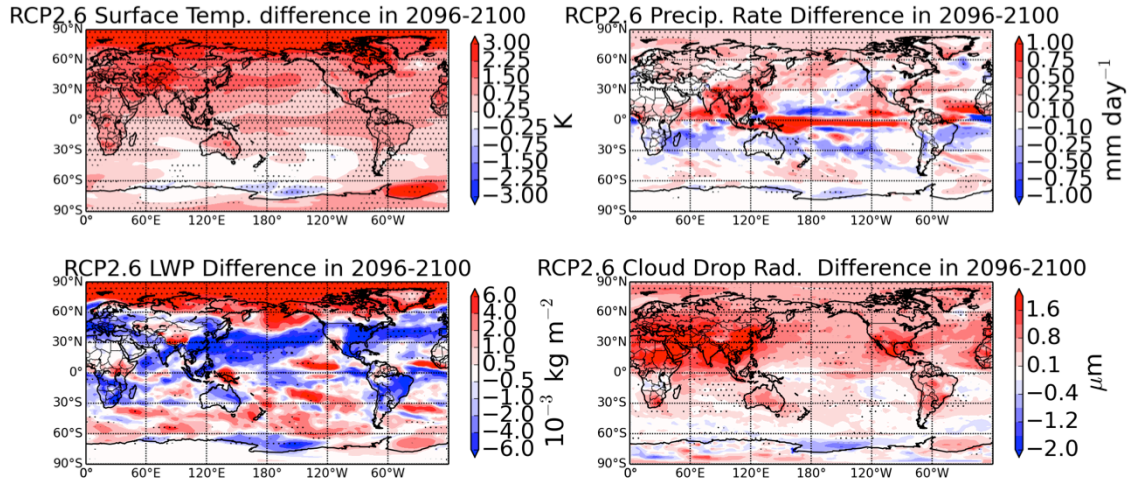


Figure S9: Changes in climate variables for a five-year average over 2096-2100 for RCP2.6. Values represent differences between the projected RCP simulations and the fixed 2005 aerosol emissions case (base case). Hatched areas represent statistically significant changes at the 95% confidence level. Upper left: surface air temperature (K) , upper right: total precipitation rate (mm day^{-1}), lower left: liquid water path (kg m^{-2}), lower right: effective cloud droplet radius at cloud top (μm)

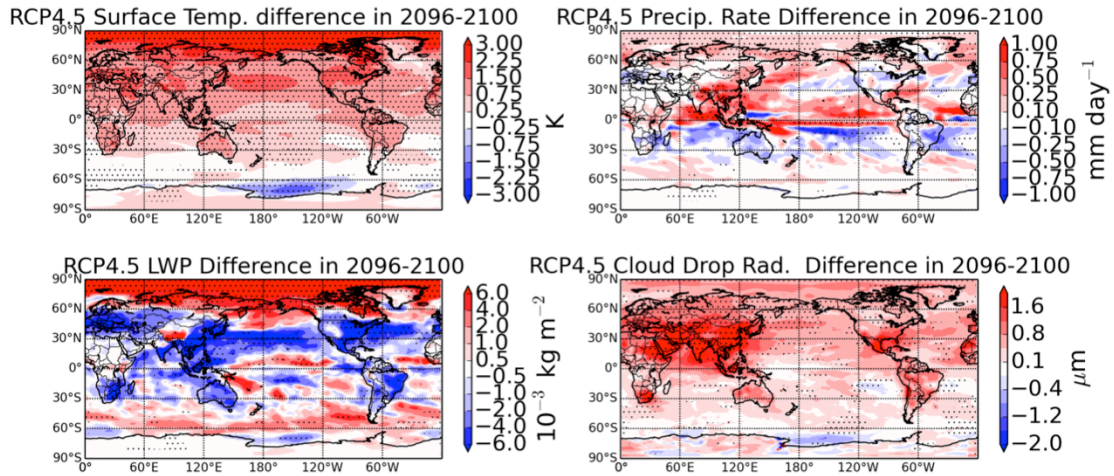


Figure S10: Changes in climate variables for a five-year average over 2096-2100 for RCP4.5. Values represent differences between the projected RCP simulations and the fixed 2005 aerosol emissions case (base case). Hatched areas represent statistically significant changes at the 95% confidence level. Upper left: surface air temperature (K), upper right: total precipitation rate (mm day⁻¹), lower left: liquid water path (kg m⁻²), lower right: effective cloud droplet radius at cloud top (μ m)

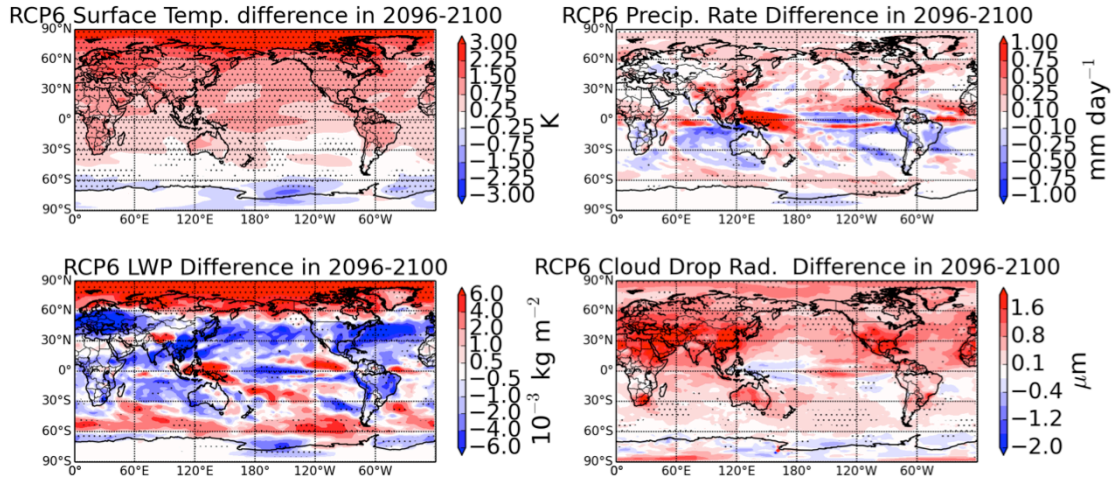


Figure S11: Changes in climate variables for a five-year average over 2096-2100 for RCP6. Values represent differences between the projected RCP simulations and the fixed 2005 aerosol emissions case (base case). Hatched areas represent statistically significant changes at the 95% confidence level. Upper left: surface air temperature (K), upper right: total precipitation rate (mm day⁻¹), lower left: liquid water path (kg m⁻²), lower right: effective cloud droplet radius at cloud top (μ m)

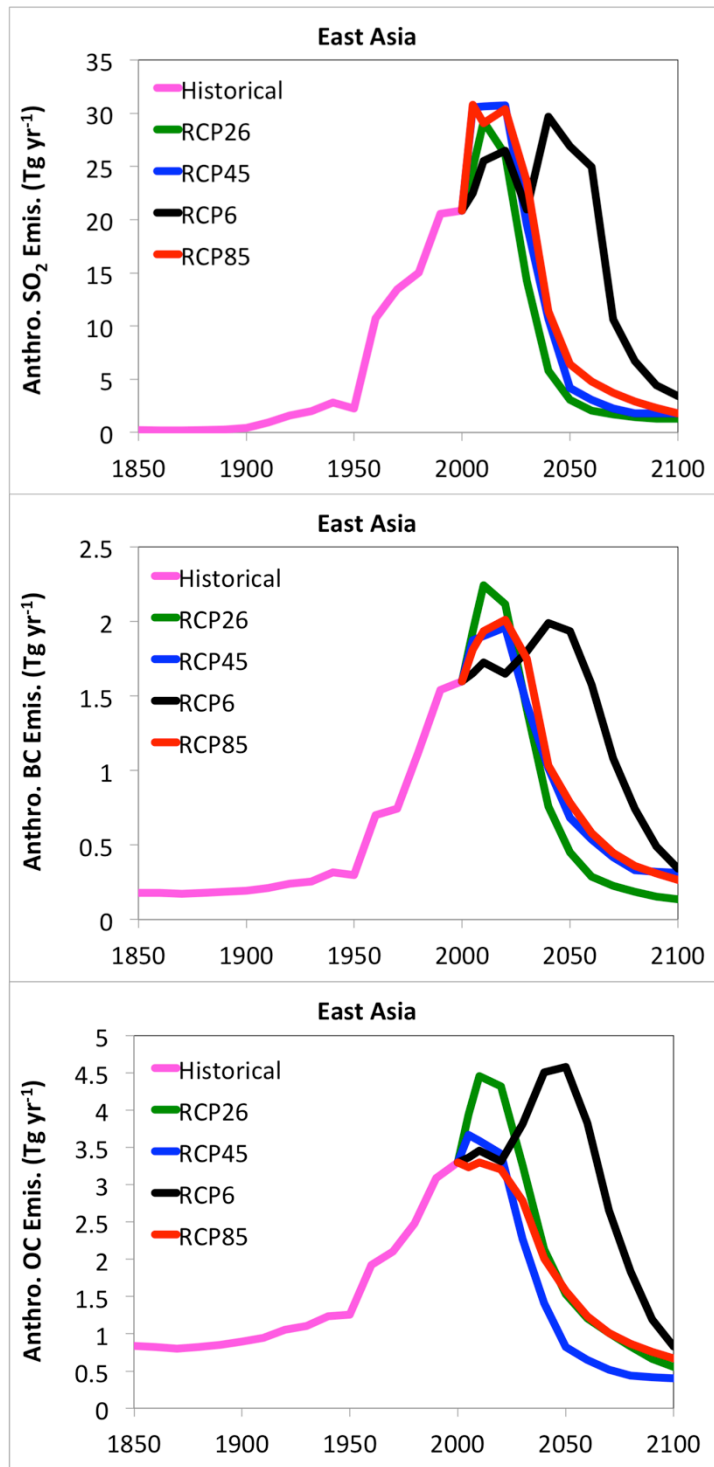


Figure S12: Sulfur dioxide, black carbon, and organic carbon anthropogenic emissions from 1860-2100 for the East Asia region. Historical emissions colored in magenta, RCP2.6 in green, RCP4.5 in blue, RCP6.0 in black, and RCP8.5 in red.

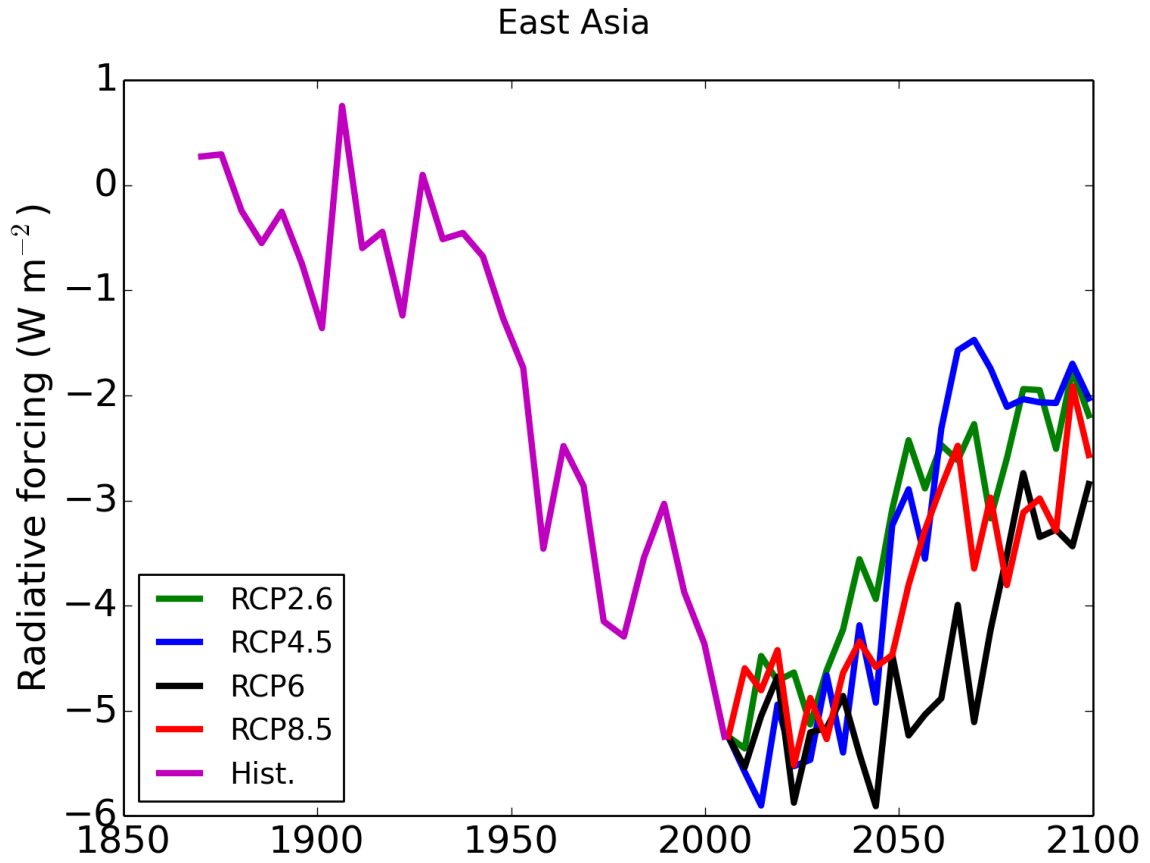


Figure S13: Top of atmosphere effective radiative forcing (ERF) in W m^{-2} for East Asia from 1860-2100 resulting from aerosol emission changes alone (versus 1860 emissions).

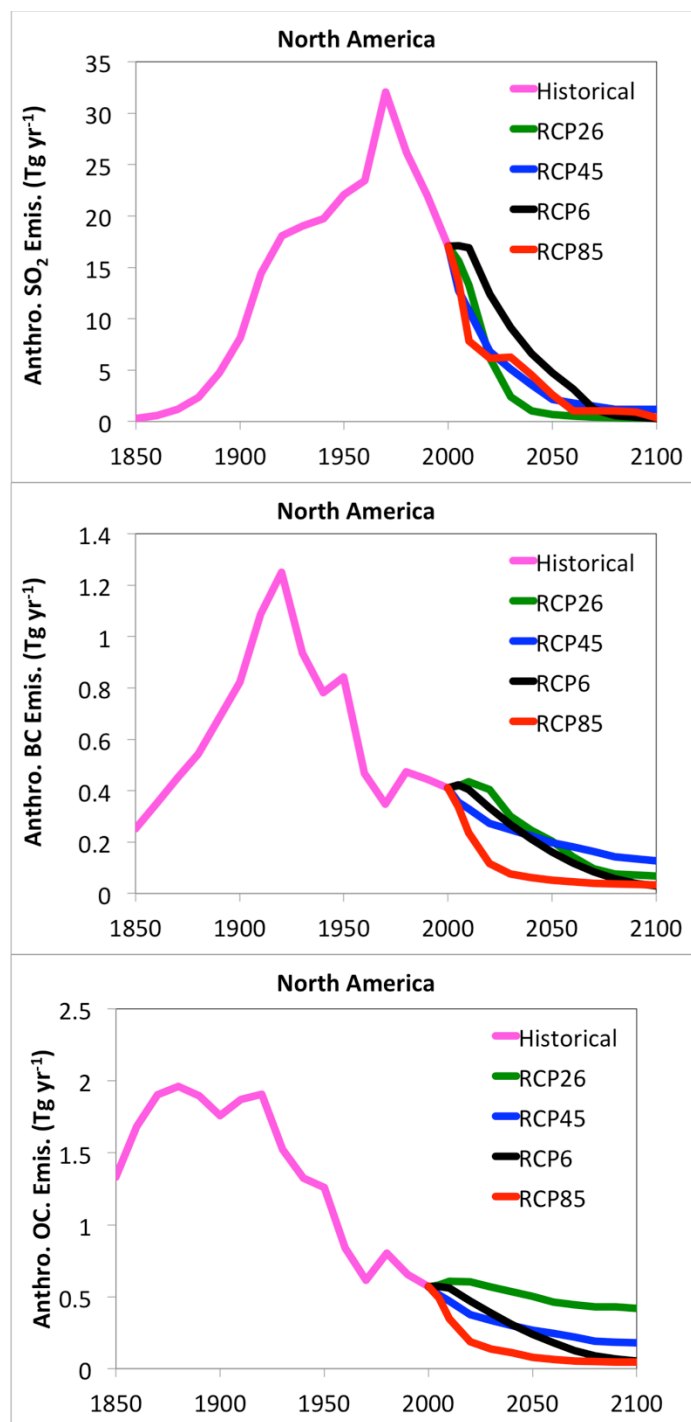


Figure S14: Sulfur dioxide, black carbon, and organic carbon anthropogenic emissions from 1860-2100 for the North America region. Historical emissions colored in magenta, RCP2.6 in green, RCP4.5 in blue, RCP6.0 in black, and RCP8.5 in red.

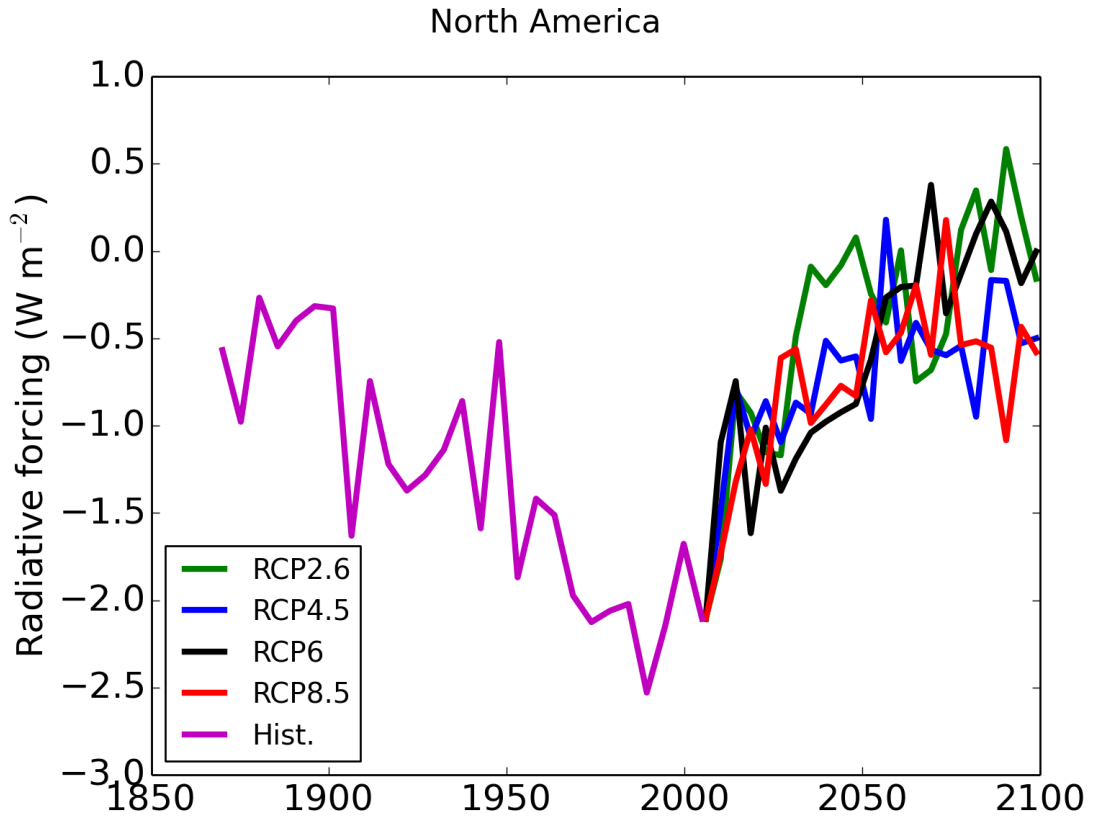


Figure S15: Top of atmosphere effective radiative forcing (ERF) in W m^{-2} for North America from 1860-2100 resulting from aerosol emission changes alone (versus 1860 emissions).

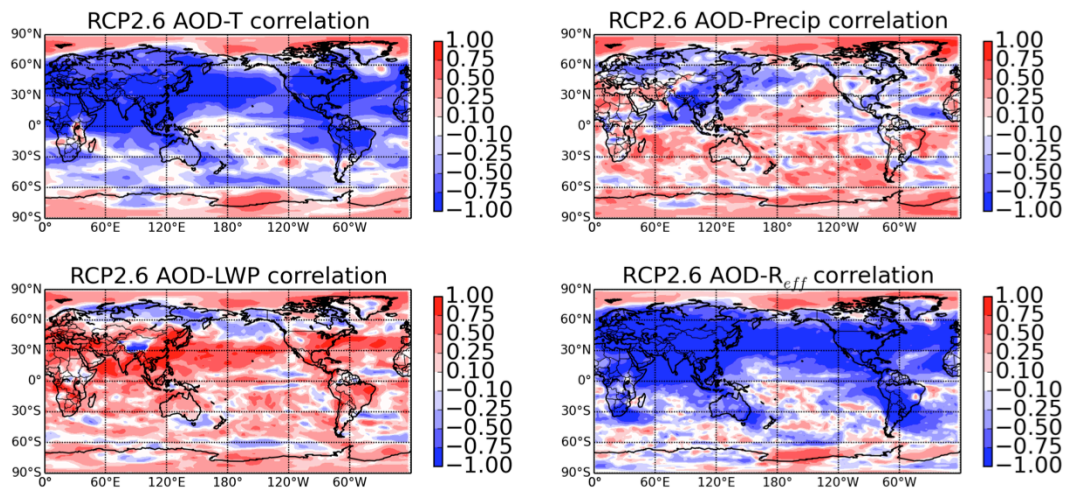


Figure S16: Correlations of aerosol-driven changes in temperature (T), precipitation rate (Precip), liquid water path (LWP), and cloud droplet radius (R_{eff}) with total anthropogenic aerosol optical depth (sulfate, black carbon, and organic carbon AOD) for RCP2.6.

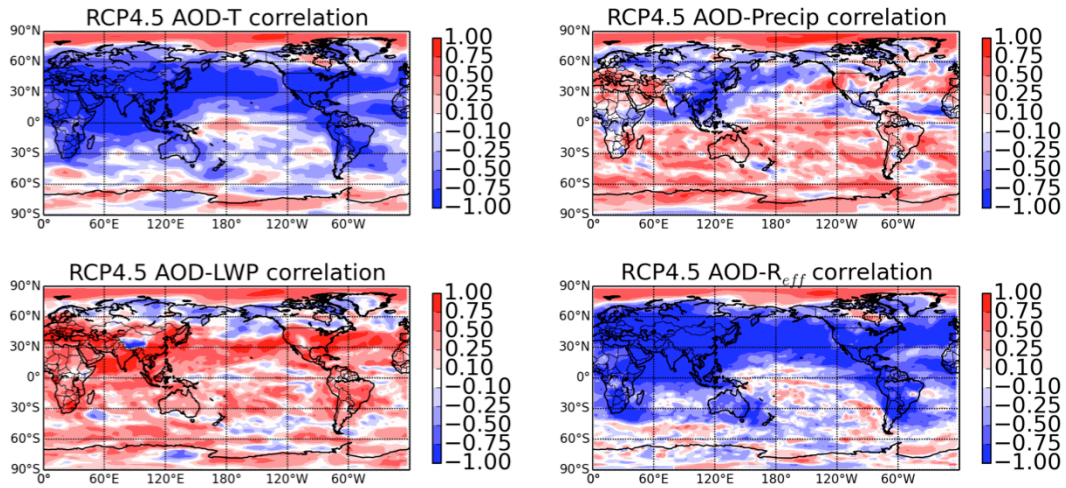


Figure S17: Correlations of aerosol-driven changes in temperature (T), precipitation rate (Precip), liquid water path (LWP), and cloud droplet radius (R_{eff}) with total anthropogenic aerosol optical depth (sulfate, black carbon, and organic carbon AOD) for RCP4.5.

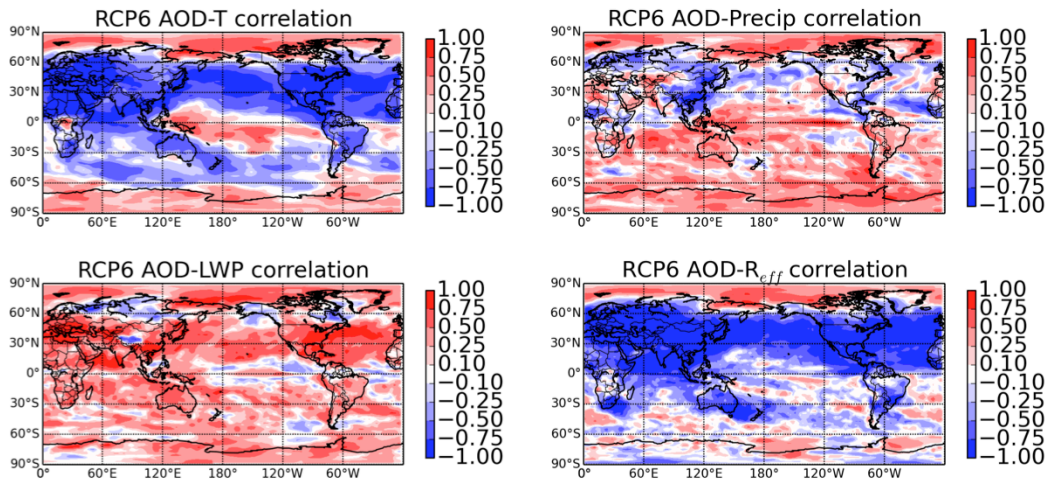


Figure S18: Correlations of aerosol-driven changes in temperature, precipitation rate, liquid water path (LWP), and cloud droplet radius (R_{eff}) with total anthropogenic aerosol optical depth (sulfate, black carbon, and organic carbon AOD) for RCP6.

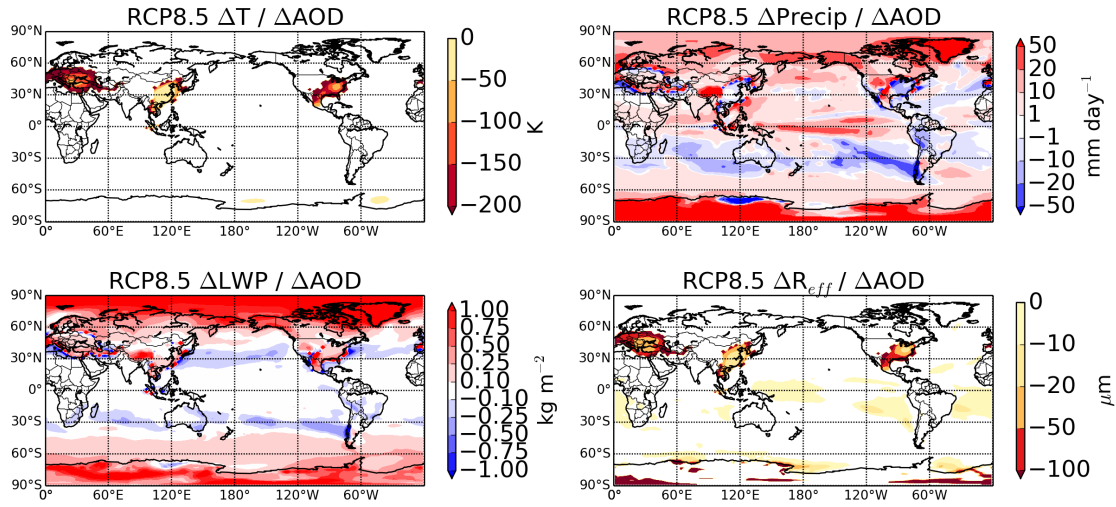


Figure S19: Ratio of change in climate parameters to change in aerosol optical depth from 2006 to 2100.

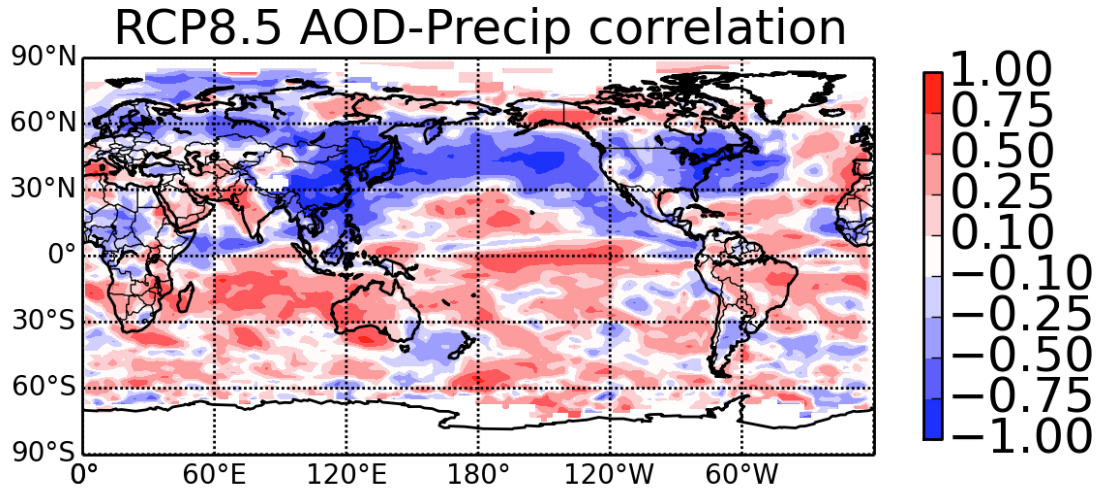


Figure S20: Correlation between aerosol driven changes in deep convective precipitation and total anthropogenic aerosol optical depth (sulfate, black carbon, and organic carbon AOD) for RCP8.5

References

Fang, Y., Fiore, A. M., Horowitz, L. W., Gnanadesikan, A., Held, I., Chen, G., Vecchi, G. and Levy, H.: The impacts of changing transport and precipitation on pollutant distributions in a future climate, , 116, 1–14, doi:10.1029/2011JD015642, 2011.

Gruebler, A. and Nakicenovic, N.: Emissions scenarios: a final response, *Energy Environ.*, 15(1), 11–24 [online] Available from: https://www.etde.org/etdeweb/details_open.jsp?osti_id=20463875 (Accessed 5 June 2014), 2004.

Manne, A. S., Richels, R. G. and Edmonds, J. A.: Market Exchange Rates Or Purchasing Power Parity: Does The Choice Make A Difference To The Climate Debate?, *Clim. Change*, 71(1-2), 1–8, doi:10.1007/s10584-005-0470-4, 2005.

Riahi, K., Grübler, A. and Nakicenovic, N.: Scenarios of long-term socio-economic and environmental development under climate stabilization, *Technol. Forecast. Soc. Change*, 74(7), 887–935, doi:10.1016/j.techfore.2006.05.026, 2007.

Riahi, K., Rao, S., Krey, V., Cho, C., Chirkov, V., Fischer, G., Kindermann, G., Nakicenovic, N. and Rafaj, P.: RCP 8.5—A scenario of comparatively high greenhouse gas emissions, *Clim. Change*, 109(1-2), 33–57, doi:10.1007/s10584-011-0149-y, 2011.

Smith, S. J., Pitcher, H. and Wigley, T. M. L.: *Future Sulfur Dioxide Emissions.*, 2005.